UDK 669.715:669.794
Original scientific article/Izvirni znanstveni članek

ISSN 1580-2949
Mater. Tehnol.

MULTIPHASE STRUCTURE AFTER HEAT TREATMENT ENABLES A SUPERIOR STRENGTH-PLASTICITY COMBINATION IN Y-MODIFIED ADC12 ALUMINUM ALLOYS

IZJEMNA KOMBINACIJA TRDNOSTI IN PLASTIČNOSTI VEČFAZNE STRUKTURE NASTALE PO TOPLOTNI OBDELAVI METAMORFNE ALUMINIJSKE ZLITINE ADC12 LEGIRANE Z ITRIJEM

Weiye Chen[1*], Linhao Liu[1], Lai Wei[1], Nan Jia[2], Guihong Geng[1]

[1]School of Material Science and Engineering, North Minzu University, Yinchuan 750021, China
[2]Key Laboratory for Anisotropy and Texture of Materials (Ministry of Education), School of Material Science and Engineering, Northeastern University, Shenyang 110167, China

Prejem rokopisa – received: 2024-09-06; sprejem za objavo – accepted for publication: 2025-06-02

doi:10.17222/mit.2024.1296

The ADC12 aluminum alloy, known for its excellent casting performance, light weight, and recyclability, is extensively utilized in the automotive industry. However, its mechanical properties still have a lot of room for improvement due to the influence of phase morphology. Rare earth Y modification and T6 heat treatment have a significant optimization effect on the mechanical properties of the alloy. During T6 heat treatment, the influence of solid solution temperature and time, as well as aging temperature and time must be comprehensively considered. This study uses orthogonal experiments to investigate the ideal heat treatment procedure for Y-modified ADC12 aluminum alloy. Microscopic structural changes after treatment are examined through deep etching and three-dimensional analysis. Our findings reveal that the microstructure is notably refined, when Si particles are reduced in size and become spherical. Additionally, most of the Al_2Cu phase dissolves into the α-Al matrix, with only a small fraction re-precipitating as fine Cu-rich particles. The optimal T6 heat treatment consists of a solutionising phase at 520 °C for 7 h, followed by artificial aging at 170 °C for 10 h. After treatment, the tensile strength reaches 332.21 MPa, and elongation is 11.6 %, indicating robust plasticity with a resilience of 3.851 GPa %. The material also exhibits a friction coefficient of 0.416 and minimal wear of 0.8 mg, signifying substantially enhanced comprehensive mechanical properties.

Keywords: ADC12 aluminum alloy, Y-modification, T6 heat treatment, deep etching, mechanical properties, orthogonal analysis

Livarska aluminijeva zlitina tipa ADC12 je znana po odličnih livnih lastnostih, lahki masi in dobrem recikliranju. Ta zlitina se pogosto uporablja v avtomobilski industriji, vendar pa se njene mehanske lastnosti še vedno lahko izboljšajo z vplivom na njeno fazno morfologijo. Redko zemeljski element itrij (Y) in izbira optimalne toplotne obdelave tipa T6 imata pomemben optimizacijski učinek na mehanske lastnostite te vrste Al zlitin. Pri toplotni obdelavi zlitine s postopkom T6 pa je treba celovito upoštevati vpliv temperature, časa zadrževanja na temperaturi homogenizacije ter temperature in časa umetnega staranja. V tem članku avtorji predstavljajo študijo uporabe ortogonalnih preizkusov za določitev idealnega postopka toplotne obdelave za izbrano aluminijevo zlitino tipa ADC12, modificirano z itrijem. Z globinskim jedkanjem nastale mikrostrukture so avtorji pregledali pod vrstičnim elektronskim mikroskopom na termično emisijo polja (TEF SEM; angl.: thermal field emission scanning electron microscope) in jo anlizirali s tridimenzionalno analizo slike. Fazno mikroanalizo so avtorji izvedli s pomočjo rentgenskega difraktometra (XRD; angl.: X-ray energy dispersive spectrometer). Avtorji ugotavljajo, da je po toplotni obdelavi nastala mikrostruktura zlitine precej spremenjena (prečiščena), delci elementarne faze Si so se dokaj zmanjšali in postali okrogli. Poleg tega se je večina faze Al_2Cu raztopila v kovinski matrici a-Al in le manjši delež se je ponovno izločil kot elementarni Cu. Optimalne lastnosti zlitine so avtorji dobili s toplotno obdelavo T6 pri kateri je potekala homogenizacija zlitine 7 ur pri 520 °C, njej pa je po hitrem ohlajanju sledilo umetno staranje zlitine 10 ur pri 170 °C. Po tej toplotni obdelavi je imela zlitina natezno trdnost cca 332 MPa in raztezek 11,6 %. To kaže na robustno plastičnost zlitine z modulom odpornosti 3851 GPa %. Material ima tudi koeficient trenja 0,416 in minimalno obrabo 0,8 mg, kar pomeni znatno izboljšane mehanskih lastnosti v celoti.

Ključne besede: livarska aluminijeva zlitina vrste ADC12, metamorfizem redkozemeljskega itrija, toplotna obdelava T6, globinsko jedkanje, mehanske lastnosti, ortogonalna analiza

1 INTRODUCTION

Al-Si alloys represent the most diverse and versatile category of cast aluminum alloys,[1] offering a high strength-to-weight ratio, excellent corrosion resistance, superior castability, high productivity, and reduced density and shrinkage.[2,3] Specifically, the ADC12 aluminum alloy has emerged as an optimal material for manufacturing critical automotive components like engine cylinder heads, blocks, and pistons due to its exceptional specific strength, corrosion resistance, as well as thermal and electrical conductivity. [4,5] Furthermore, ADC12 alloy's recyclability significantly diminishes environmental pollution and energy consumption. [6] However, the mechanical properties of recycled aluminum alloys are frequently compromised by the morphology of phases within the al-

*Corresponding author's e-mail:
wychen_neu@163.com (Weiye Chen)

Table 1: ADC12 aluminum alloy chemical composition

Element	Si	Fe	Cu	Mn	Mg	Ni	Zn	Sn	Pb	Al
w/%	9.6-12.0	≤0.85	1.8-3.5	≤0.5	≤0.3	≤0.5	≤0.95	≤0.1	≤0.1	Bal.

loys, particularly the Si matrix and impurity iron phases. Large or needle-like phases can critically weaken the matrix, diminishing the strength and ductility of an alloy, thus restricting its applications.[7] The matrix Si phase, inherently brittle, tends to form rough flake- or needle-like structures in the as-cast state, exacerbating stress concentration and degrading mechanical properties, particularly elongation and fracture toughness.[8,9] An excessively impure Fe content fosters the formation of coarse-grained, Fe-rich intermetallics, including acicular β-Al_5FeSi, which serve as prominent cracking sources.[10] Large acicular Fe phases detrimentally impact the mechanical properties of cast Al-Si alloys due to the stress concentrations at the interfaces between significant hard phases and the matrix, further instigating initial crack formation.[11] Thus, enhancing the mechanical properties of cast Al-Si alloys necessitates effective strategies to mitigate or modify these deleterious phases and improve the matrix phases.

A. Jarco et al.[12] explored the influence of AlSi11 (solution treatment and artificial aging) on the mechanical properties and microstructural alterations of AlSi11 (Fe) alloys, finding that the eutectic Si phase partially spheroidized and solidified after heat treatment, compared to its initial state. C. Rungsinee et al.[13] identified the optimal solid solution treatment conditions for ADC12 alloys as 520 °C for 8 h, with artificial aging at 170 °C for 6 h, significantly enhancing mechanical properties through refinement of the acicular eutectic structure. The primary, and secondary reinforcing phases in ADC12 alloys, the eutectic Si and iron-rich phases, can be refined by adding rare earth elements to them.[14] Li M. Wang et al.[15] demonstrated that the mechanical properties of ADC12 aluminum alloys improve with the addition of rare earth elements, particularly yttrium (Y), which notably refines the grain structure and enhances high-temperature tensile properties in Al-5 *w*/% Cu-based alloys by reducing the volume of eutectic crystals and shortening the crystallization range. However, the impact of the T6 heat treatment on improving the mechanical properties of die-cast ADC12 regenerated aluminum alloy remains limited. Our previous studies show that with a 0.1-% addition of rare earth Y, the Si and Fe phases are optimally refined, their detrimental impact on the matrix is significantly reduced and the comprehensive mechanical properties improved.[16] On this basis, applying heat treatment is expected to enable a superior strength-plasticity balance.

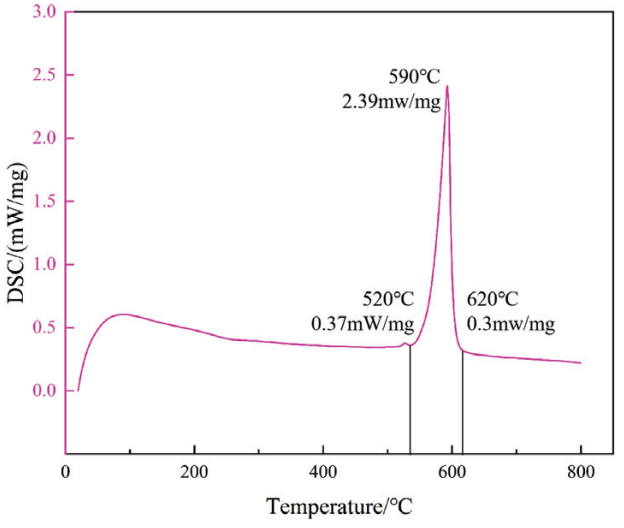

Figure 1: DSC curve of ADC12 aluminum alloy

2 EXPERIMENT

2.1 Materials

The experiment utilized commercial ADC12 aluminum alloy, with its principal components detailed in **Table 1**. Employing an Al-20 *w*/% Y intermediate alloy, a 0.1 *w*/% rare-earth modified ADC12 recycled aluminum alloy was synthesized for the experiment after the content calculation. The sample designated for heat treatment was produced via centrifugal casting using a small vacuum high-frequency induction-melting furnace.

2.2 Methods

The experimental heat treatment regimen was designed based on the orthogonal principle.[17] This study aimed to determine the optimal heat treatment process for enhancing the mechanical properties of rare-earth Y-metamorphic centrifugal casting of ADC12 aluminum alloy. An orthogonal array of $L_9(3^4)$ was employed to streamline the optimization of the heat treatment parameters, detailed in **Table 2**. While several factors influence the efficacy of heat treatment, the solid solution temperature and duration are typically considered crucial, exerting the most pronounced impact. Differential thermal analysis indicated the lowest phase transition temperature for the ADC12 alloy to be 525 °C, as depicted in **Figure 1**. To prevent any phase transformations during the solid solution treatment, a maximum temperature of 520 °C was meticulously selected.

The T6 heat treatment applied to the castings involved a solid solution treatment with a temperature increase rate of 10 °C/min, followed by quenching in 60 °C water for 15 s, and artificial aging in a dry box for 5 min. The optimal heat treatment process, selected

Table 2: T6 heat treatment parameters

Groups	Horizontal combination	Solid solution temperature/°C	Solid solution time/h	Aging temperature /°C	Aging time /h
1	$A_1B_1C_1D_1$	500	5	160	6
2	$A_1B_2C_2D_2$	500	6	170	8
3	$A_1B_3C_3D_3$	500	7	180	10
4	$A_2B_1C_2D_3$	510	5	170	10
5	$A_2B_2C_3D_1$	510	6	180	6
6	$A_2B_3C_1D_2$	510	7	160	8
7	$A_3B_1C_3D_2$	520	5	180	8
8	$A_3B_2C_1D_3$	520	6	160	10
9	$A_3B_3C_2D_1$	520	7	170	6

based on its superior tensile strength, was employed for verification experiments. The samples subjected to this optimal treatment included verification groups, identified using an analysis of tensile strength extremes.

Metallographic samples were polished and etched using an erosive agent (HF+HCl+HNO_3+H_2O). A quantitative analysis of the phase organization within the alloy was conducted using Image-Pro Plus software. Room temperature tensile experiments were performed with a CMT5053 universal testing machine, in accordance with GBT7314-2017, at a tensile rate of 0.6 mm/min. ZEISS Vert A1 type optical metallographic microscope was used to observe and analyze the metallographic structures of the samples. The ZEISS Sigma500 thermal field emission scanning electron microscope (SEM) was used to analyze the microstructures of the samples, and an Oxford Aztec X50Max X-ray energy dispersive spectrometer (EDS) was equipped to analyze the contents of different elements in the samples. A DSC analysis was performed using a German NETZSCH STA 449 F3 differential scanning calorimeter.

3 EXPERIMENTAL RESULTS

3.1 Effect of T6 heat treatment on micro-organization of Y-modified ADC12 aluminum alloy

Metallographic images (**Figures 2a** to **2d**) illustrate the microstructural transformations in the Y-modified

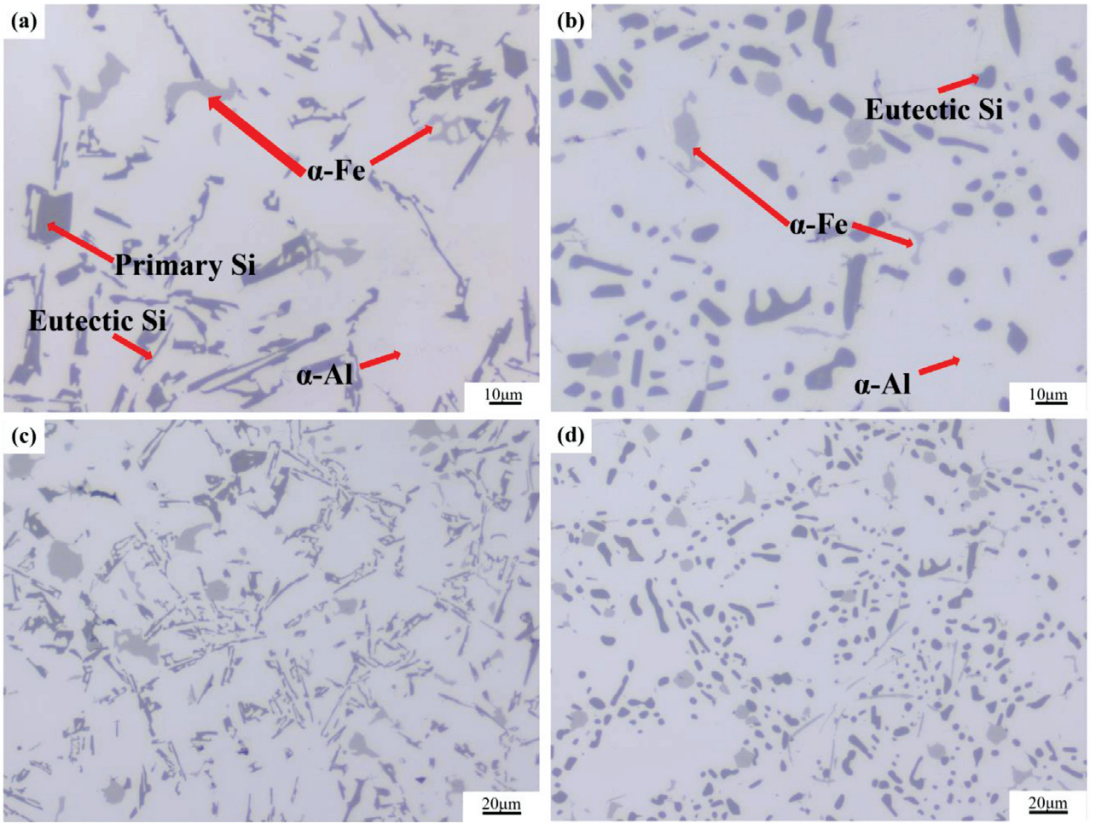

Figure 2: Metallographic microstructure of Y-phase-modified ADC12 aluminum alloy before and after heat treatment: a), c) not heat-treated; b), d) validation experimental group

ADC12 aluminum alloy before and after heat treatment. Initially, the α-Al matrix appears as large, irregular white regions without a defined outline. After treatment, it transforms into a supersaturated solid solution with a clearer and more uniform distribution, and with a noticeable increase in the area percentage. The large irregular polygonal dark black structures, representing the incipient Si phase, nearly vanish after heat treatment. The remaining dark-black structures, characteristic of the eutectic Si phase, initially appear as large flakes and fibrous forms with numerous branches and crystalline grooves, serving as cutting points within the matrix. After treatment, these edges are noticeably blunted, appearing spherical or as short rods. The α-Fe phase, characterized by a light-gray, kanji-like, herringbone, and irregular polygonal morphology – commonly identified as α-$Al_{25}(FeMn)_3Si_2$ – undergoes minimal morphological alteration during heat treatment; however, the size is notably reduced, and the edges become blunted. The morphology, size, and distribution of these phase structures profoundly influence the properties of the alloy, with the shape, size, and distribution of incipient Si and eutectic Si, along with the dissolution and precipitation of Al_2Cu, being critical factors affecting the alloy's characteristics.[18–20]

3.1.1 Effect of heat treatment on the α-Al phase

Figure 3 vividly illustrates the microstructural evolution of the rare earth Y-modified ADC12 aluminum alloy, captured through deep etching before and after heat treatment. Initially, most of the α-Al matrix appears as coarse, tree-like dendrites. Following heat treatment, a significant transformation occurs due to the solid dissolution of numerous soluble elements within the α-Al matrix, altering its crystal structure. This change results in parts of the α-Al matrix converting into irregular blocks. However, remnants of the matrix retain the form of fine dendritic crystals, highlighting the differential effects of the heat treatment across the matrix.

3.1.2 Effect of heat treatment on the Si phase

Figure 4 shows secondary electron images of the eutectic Si phase in the Y-modified ADC12 aluminum alloy, captured before and after extensive etching and heat treatment. Before heat treatment, the eutectic Si phase predominantly appears as lumps and laminae with highly irregular shapes and pronounced angles. These formations exhibit a notable cutting effect on the matrix, significantly impacting the mechanical properties of the alloy. After heat treatment, the eutectic Si phase undergoes a substantial transformation into shorter rods; this change includes a notable reduction in size and a spheroidization of the edges. The heat-treatment process

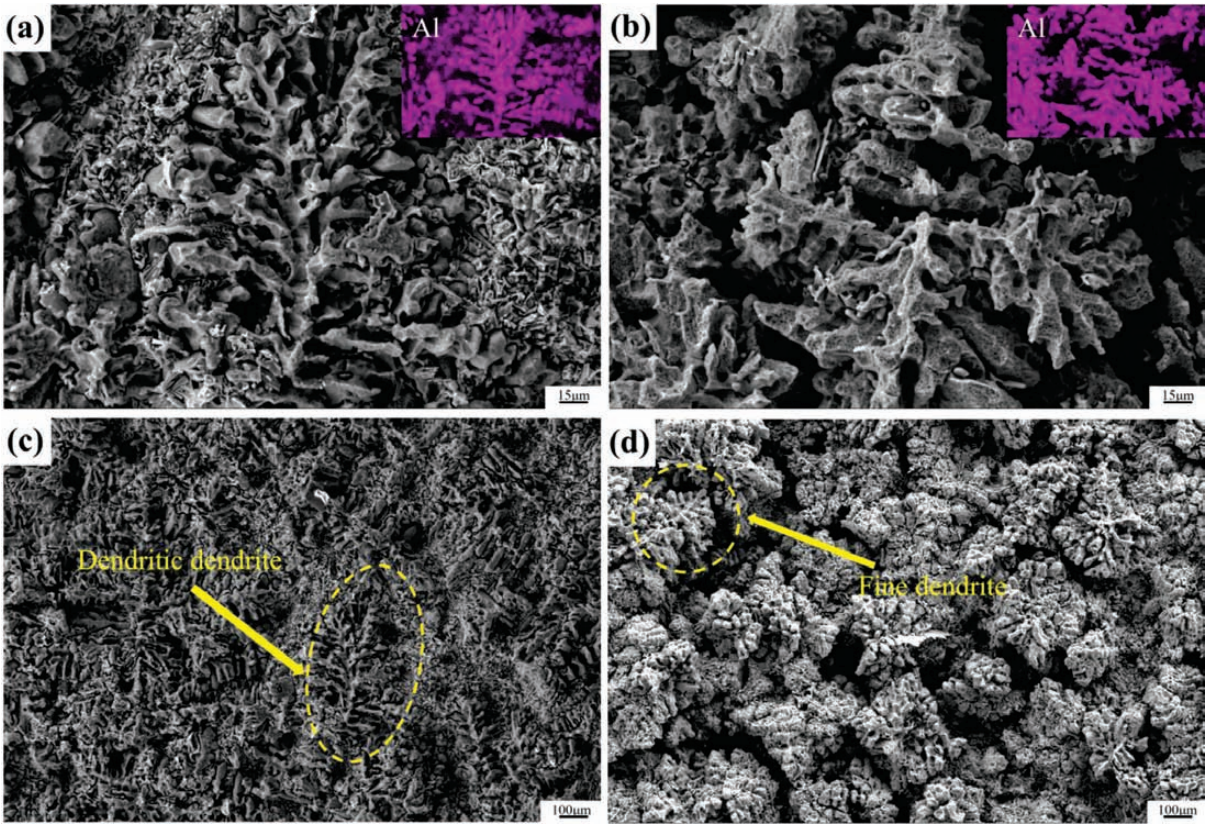

Figure 3: Secondary electron images of deeply etched surface of Y-phase-modified ADC12 aluminum alloy before and after heat treatment: a), c) not heat-treated; b), d) validation experimental group

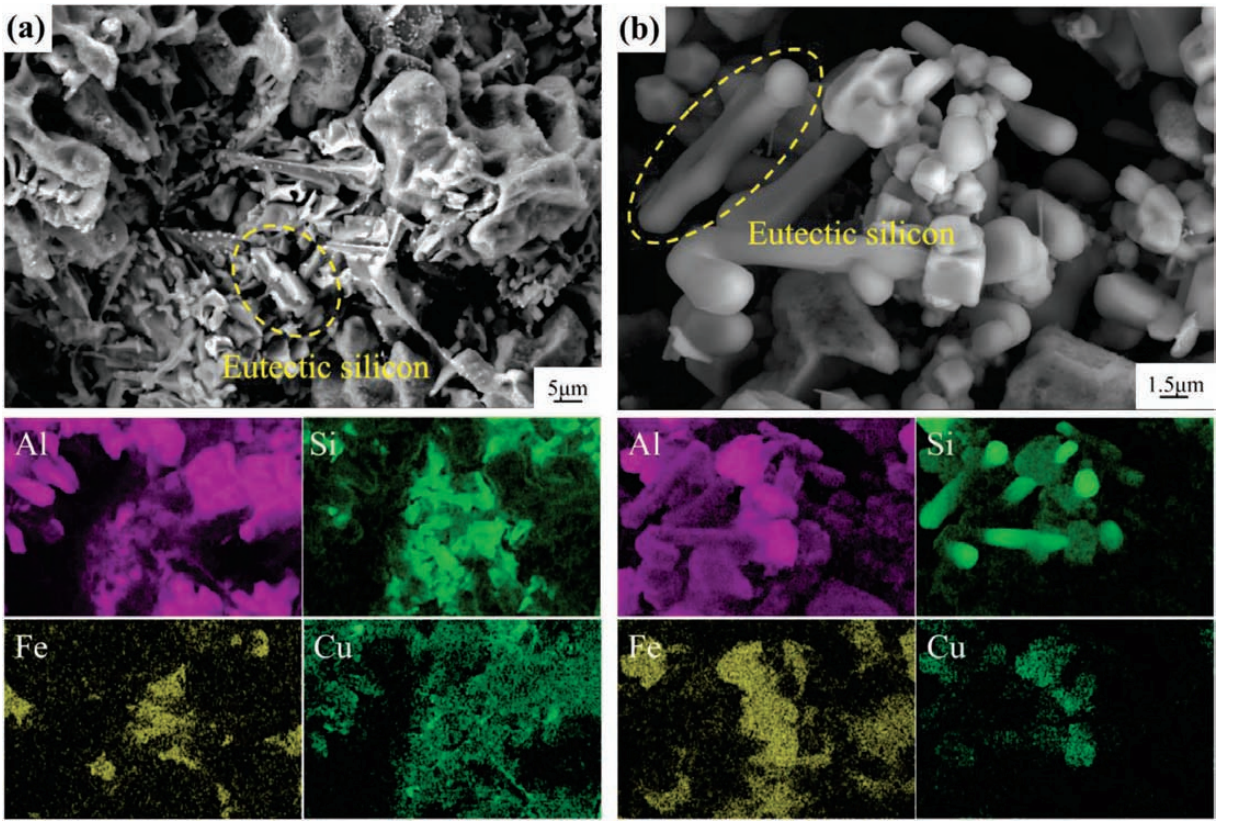

Figure 4: Secondary electron images of eutectic Si phase of Y-phase-modified ADC12 aluminum alloy after deep etching before and after heat treatment: a) not heat-treated; b) validation experimental group

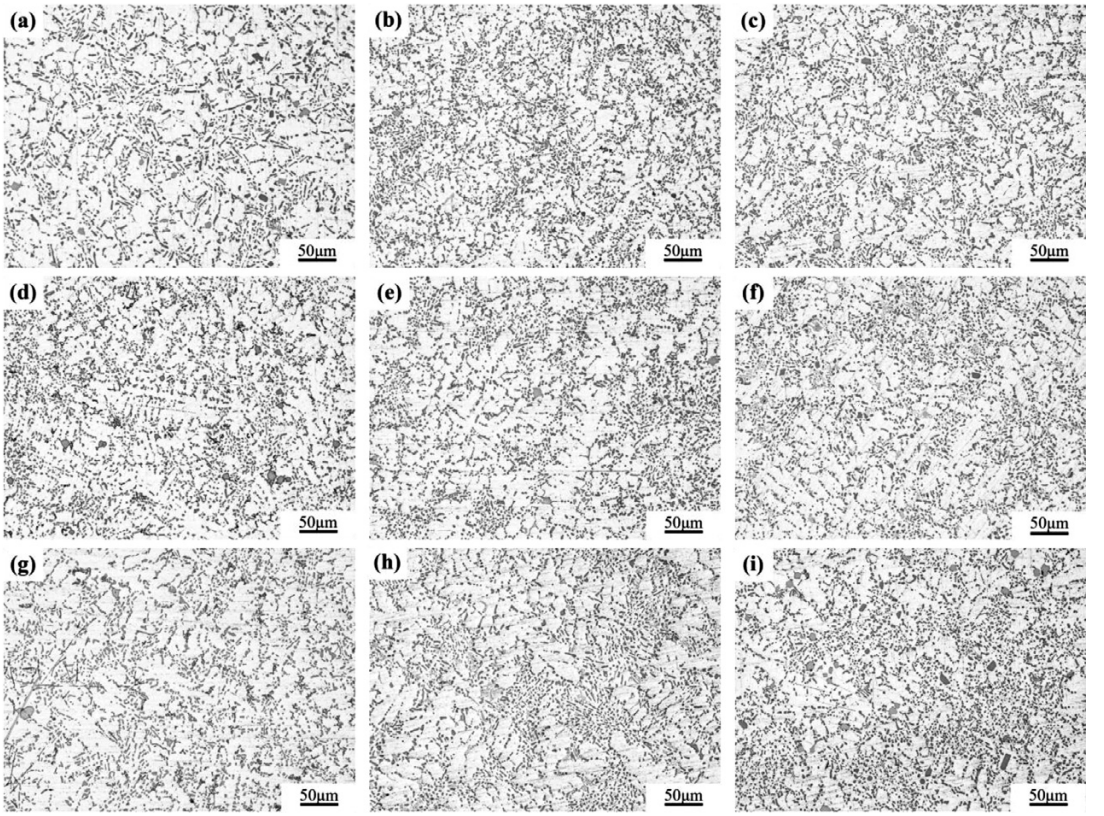

Figure 5: Metallographic microstructure of Y-modified ADC12 aluminum alloy with different heat treatment parameters: a) Group 1; b) Group 2; c) Group 3; d) Group 4; e) Group 5; f) Group 6; g) Group 7; h) Group 8; i) Group 9

thus significantly influences the morphology of the Si phase, improving the alloy's structural integrity and potentially enhancing its mechanical performance.

Figure 5 shows the metallographic microstructure of the Y-modified ADC12 aluminum alloy subjected to various heat treatment parameters. The eutectic Si experiences dissolution and fracture at certain branches and grooves, intensified with rising temperatures, leading to further dissolution of the Si phase into the α-Al matrix. As the solid solution treatment extends to 5 h, the eutectic Si phase shows signs of dissolution and initial breakage. After 6 h, this breakage is complete, accompanied by noticeable spheroidization. After 7 h, the eutectic Si spheroidization is fully achieved, with a visible tendency for growth if the holding time is further prolonged. This significant coarsening of the eutectic Si with extended holding times reduces the alloy's strength.

During the solid solution treatment, part of the Si phase dissolves into the α-Al matrix, leaving the residual eutectic Si phase more evenly distributed and markedly spheroidized, with most precipitated Si particles appearing relatively rounded. A 5-h solid solution treatment results in uneven Si phase sizes and predominantly elongated rods in groups 1, 4, and 7, indicating that as eutectic Si dissolution has occurred, spheroidization is incomplete. After 7 h, the eutectic Si phase in groups 3, 6, and 9 shows varying sizes and some growth, suggesting coarsening under these conditions. The aging treatment at 160 °C for groups 1, 6, and 8 leads to a very uneven distribution of the Si phase, highlighting a low degree of homogenization under these conditions.

It is evident from **Figure 5** that the parameters of the solid solution and aging treatments significantly influence the alloy's microstructure. With increasing solid solution temperature and duration, the Si phase content in the samples decreases. However, excessively prolonged solid solution times can induce growth in the Si phases. Similarly, as the aging temperature and duration increase, the reinforcement phase dissolved in the matrix begins to precipitate, and with the spheroidization of the Si phase, the reinforcement phase is completed, enhancing the alloy's strength and hardness. However, excessive aging conditions can promote growth in the precipitated Si particles, potentially diminishing the alloy's strength.

Figure 6 presents an analysis of the phase area percentage, average aspect ratio, and average size of the Si phase in Y-modified ADC12 aluminum alloy before and after heat treatment. After heat treatment, the area percentage of the Si phase in the sample decreased from 20.48 % to 14.78 %, which is a reduction of 27.83 %. This confirms that a significant portion of the Si phase has dissolved into the α-Al matrix, showcasing the efficacy of the solid solution treatment. Additionally, the average aspect ratio of the Si phase dropped from 3.43 to 2.06, representing a 39.94 % decrease, and indicating successful spheroidization during heat treatment. The average size of the Si phase shrank markedly from 24.13 μm² to 10.16 μm², which is a reduction of 57.89 %, highlighting the refining effect of heat treatment.

Figure 7 depicts the size distribution of the Si phase in the Y-modified ADC12 aluminum alloy before and after heat treatment. After treatment, most Si phase sizes in the samples are under 5 μm², substantially reducing larger Si phases of over 50 μm² and completely eliminating those over 100 μm². This comparative analysis reveals that the significant reduction in the Si phase area after T6 heat treatment enhances the solid solution saturation of Si in the α-Al matrix, forming a supersaturated solid solution. During the subsequent aging process, re-precipitation of the Si phase begins, indicating dynamic changes in the microstructure that influence the alloy's properties.

3.1.3 Effect of heat treatment on the α-Fe phase

Figure 8 illustrates the changes in the area share, average size, and average aspect ratio of the α-Fe phase in

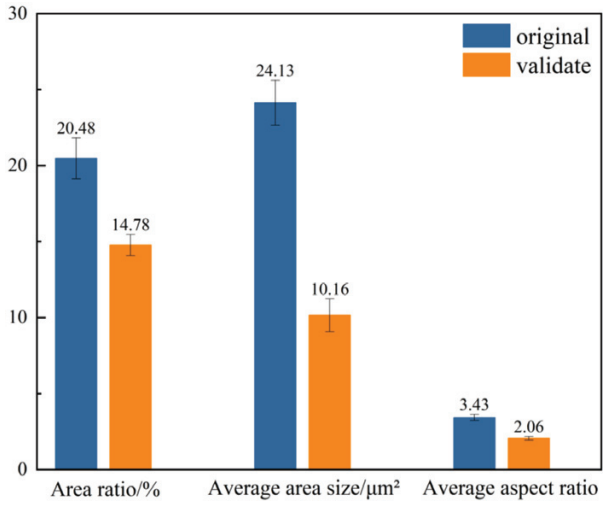

Figure 6: Si-phase area share, average size, and average aspect ratio of Y-modified ADC12 aluminum alloy before and after heat treatment

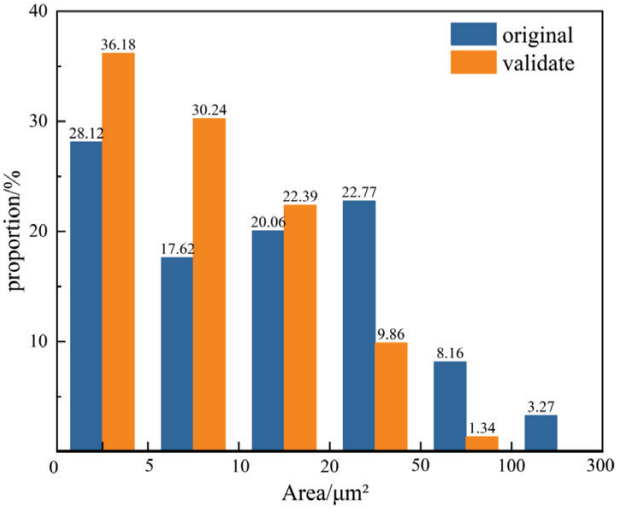

Figure 7: Si-phase size distribution in Y-modified ADC12 aluminum alloy before and after heat treatment

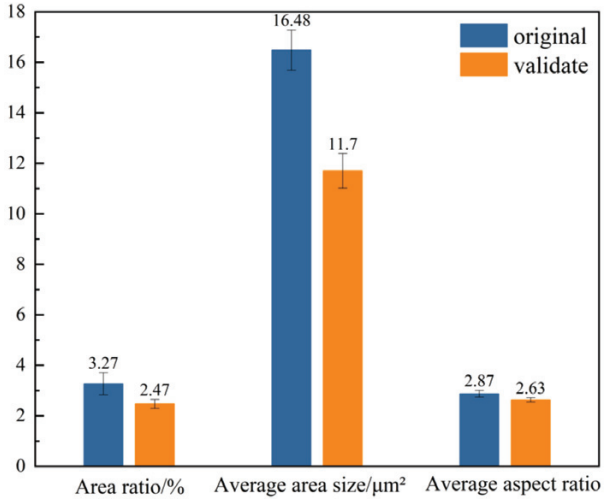

Figure 8: Area share, average size, and average length-to-diameter ratio of α-Fe phase in Y-modified ADC12 aluminum alloy before and after heat treatment

Y-modified ADC12 aluminum alloy before and after heat treatment. The most notable post-heat-treatment alteration is observed in the average size of the α-Fe phase, which decreased from 16.48 μm² to 11.7 μm² – a 29.00 % reduction compared to pre-heat-treatment samples. This reduction validates the effectiveness of heat treatment in refining the α-Fe phase, although its impact on the phase's morphology remains limited. This limited morphological change is likely due to the incorporation of rare earth Y, which shortens the alloy's solidification time, enhances the nucleation rate, and consequently refines the size of the iron-rich phase. Additionally, the chosen solid-solution temperature, being lower than the melting temperature of the α-Fe phase,[21] and the substantial atomic size difference between Fe and Al hinder the dissolution of the iron-rich phase into the matrix. In the absence of external energy input, and despite prolonged holding times, the bonding between Fe atoms and their surrounding constituents remains largely unaffected.

3.1.4 Effect of heat treatment on the Al_2Cu phase

Figure 9 shows secondary electron images of the alloy before and after heat treatment, revealing a transformation in the Si phase from flaky and striped forms to short rods and spheres according to the energy spectrum analysis. The brighter regions in these images represent the Al_2Cu phase. After solid-solution treatment, most of the Al_2Cu phase is dissolved into the α-Al matrix, making it virtually invisible on the alloy's surface. A deeply etched alloy sample is utilized to facilitate this observation.

Figure 10a shows a secondary electron image of the alloy prior to heat treatment, where the Al_2Cu phase appears as spherical precipitates attached to the α-Fe phase. **Figure 10b** includes a post-heat-treatment image, showing tiny white dots associated with the eutectic Si phase; these dots represent Cu precipitates formed during heat treatment. As most of the Al_2Cu phase dissolves in the α-Al matrix during heat treatment, and only a minor portion of Cu atoms precipitate, both the size and oc-

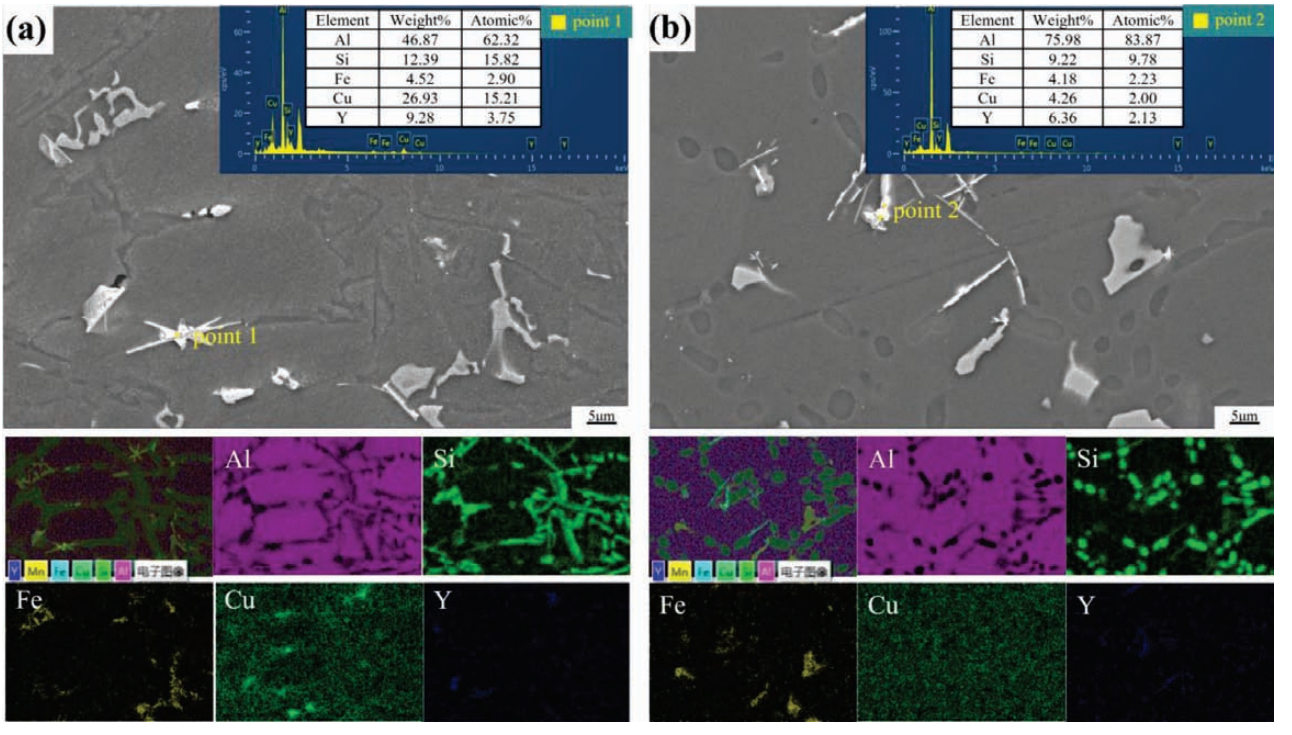

Figure 9: Secondary electron images of Y-modified ADC12 aluminum alloy before and after heat treatment: a) without heat treatment; b) validation experimental group

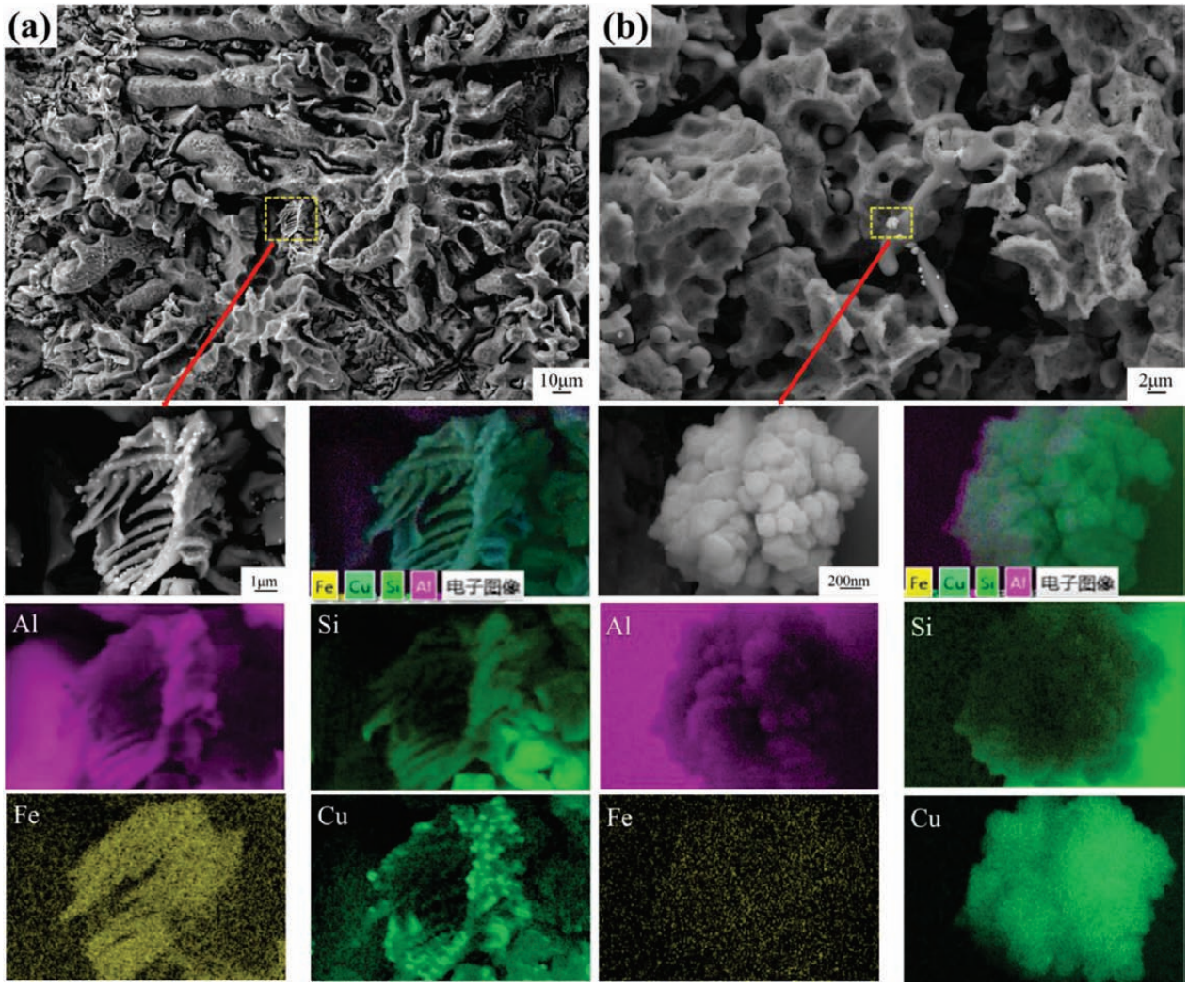

Figure 10: Deeply etched secondary electron images of the Cu phase of Y-modified ADC12 aluminum alloy before and after heat treatment: a) without heat treatment; b) validation experimental group

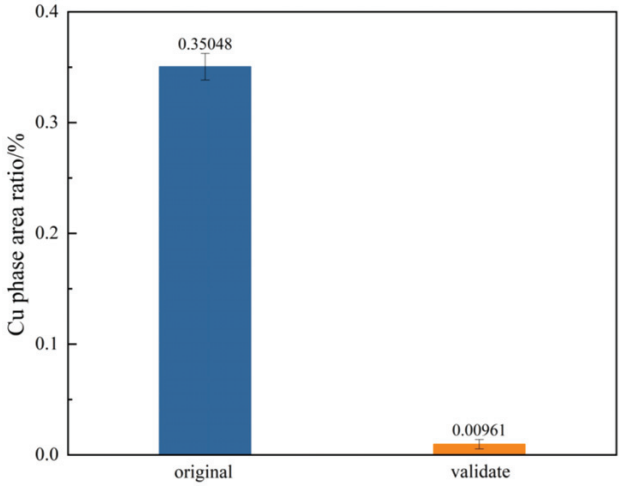

Figure 11: Area fraction of the Cu phase in Y-modified ADC12 aluminum alloy before and after heat treatment

currence frequency of the Cu phase are significantly diminished.

Figure 11 illustrated the measurement of the Cu phase area, further underscoring these transformations, showing a reduction from 0.35048 to 0.00961 % after heat treatment – a 97.26-% decrease compared to the pre-heat treatment sample. This dramatic reduction corroborates the effectiveness of the solid solution treatment in dissolving the Al_2Cu phase, confirming its significant impact on the alloy's microstructure.

3.2 Effect of T6 heat treatment on the mechanical properties of Y-modified ADC12 aluminum alloy

3.2.1 Tensile properties

Figure 12 displays the tensile strength, elongation, and strength-plasticity product of the ADC12 alloy subjected to various T6 heat treatment processes. The data reveal that the tensile strength of the orthogonal validation group surpasses that of all other orthogonal test groups, affirming the validity of this experimental design.

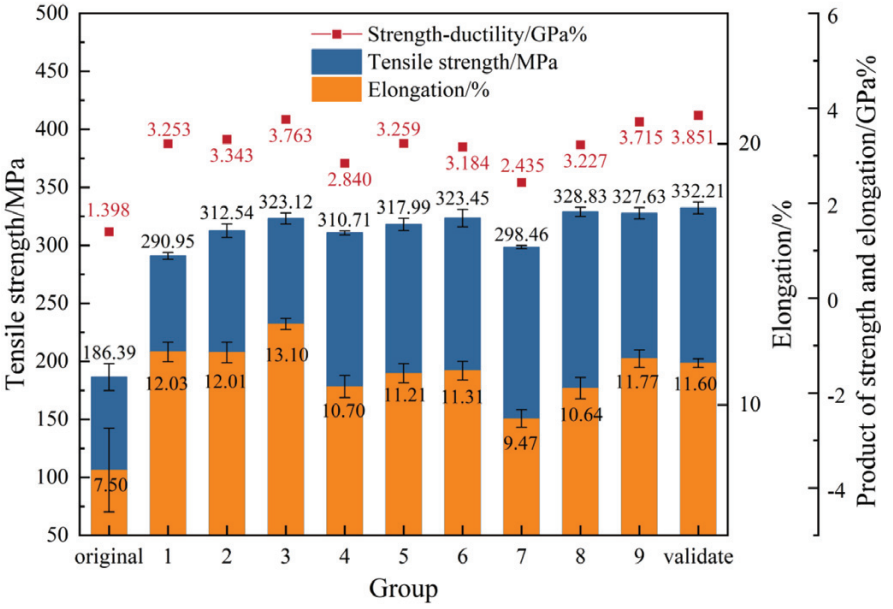

Figure 12: Tensile strength, elongation, and a high strength-plasticity product of ADC12 alloy under different T6 heat treatment processes

Table 3: Analysis of extreme differences in tensile strength during T6 heat treatment

Groups	Horizontal combination	Solid solution temperature/°C	Solid solution time/h	Aging temperature/°C	Aging time/h	Tensile strength/MPa
1	$A_1B_1C_1D_1$	500	5	160	6	290.95
2	$A_1B_2C_2D_2$	500	6	170	8	312.54
3	$A_1B_3C_3D_3$	500	7	180	10	323.12
4	$A_2B_1C_2D_3$	510	5	170	10	310.71
5	$A_2B_2C_3D_1$	510	6	180	6	317.99
6	$A_2B_3C_1D_2$	510	7	160	8	323.45
7	$A_3B_1C_3D_2$	520	5	180	8	298.46
8	$A_3B_2C_1D_3$	520	6	160	10	328.83
9	$A_3B_3C_2D_1$	520	7	170	6	327.63
k1		926.61	900.12	943.23	936.57	
k2		952.15	959.36	950.88	934.45	
k3		954.92	974.20	939.57	962.66	
K1		308.87	300.04	314.41	312.19	
K2		317.38	319.79	316.96	311.48	
K3		318.31	324.73	313.19	320.89	
R		9.44	24.69	3.77	9.40	

Specifically, compared to the non-heat-treated sample, the tensile strength significantly increased from 186.39 MPa to 332.21 MPa, marking a 78.23 % improvement over the pre-heat-treatment sample; the elongation also rose from 7.50 to 11.60 %, which was a 54.67 % increase relative to the pre-heat-treatment sample. Furthermore, the product of strength and plasticity showed a remarkable enhancement, escalating from 1.398 GPa % to 3.851 GPa %, which was an increase of 175.46 %. This substantial rise reflects the optimal balance between strength and plasticity achieved through the heat treatment process, showcasing the effectiveness of the T6 treatment in enhancing both mechanical properties of the ADC12 alloy.

Table 3 outlines the impact of various T6 heat treatment factors on the tensile strength of the alloy, ranking their influence as follows: solid solution time>solid solution temperature>artificial aging time>artificial aging temperature. The optimal heat treatment conditions, identified through orthogonal testing and subsequent calculations to maximize tensile strength, include a solid solution temperature of 520 °C, solid solution time of 7 h, artificial aging temperature of 170 °C, and aging time of 10 h. These parameters closely align with the process that maximizes the degree of solid solution of the Si phase, suggesting that the extent of Si phase dissolution and homogenization significantly influences the mechanical properties of the alloy.

As can be seen from **Table 4**, the influence of the four T6 heat treatment parameters on elongation follows the order: solid solution time > solid solution temperature > artificial aging time > artificial aging temperature.

Table 4: Analysis of extreme differences in elongation during T6 heat treatment

Groups	Horizontal combination	Solid solution temperature/°C	Solid solution time/h	Aging temperature/°C	Aging time /h	Elongation /%
1	$A_1B_1C_1D_1$	500	5	160	6	11.18
2	$A_1B_2C_2D_2$	500	6	170	8	10.70
3	$A_1B_3C_3D_3$	500	7	180	10	11.65
4	$A_2B_1C_2D_3$	510	5	170	10	9.14
5	$A_2B_2C_3D_1$	510	6	180	6	10.25
6	$A_2B_3C_1D_2$	510	7	160	8	9.84
7	$A_3B_1C_3D_2$	520	5	180	8	8.16
8	$A_3B_2C_1D_3$	520	6	160	10	9.82
9	$A_3B_3C_2D_1$	520	7	170	6	11.34
k1		33.52	28.48	30.84	32.77	
k2		29.23	30.76	31.18	28.70	
k3		29.32	32.83	30.06	30.60	
K1		11.17	9.49	10.28	10.92	
K2		9.74	10.25	10.39	9.57	
K3		9.77	10.94	10.02	10.20	
R		1.40	1.45	0.37	1.36	

This ranking is consistent with the corresponding influence hierarchy for tensile strength. The orthogonal test and the above calculations show that the heat treatment parameters used to obtain the best elongation rate include a solid solution temperature of 500 °C, solid solution time of 7 h, artificial aging temperature of 170 °C, and aging time of 6 h.

Figure 13 illustrates the fracture morphology of the Y-modified ADC12 aluminum alloy before and after heat treatment. Prior to treatment, the fracture surface predominantly exhibits a decohesive fracture mode, with crack propagation along the grain boundaries of varying orientations. The fracture surface is characterized by decohesive regions interspersed with microcracks and sporadic tearing ridges, indicating a brittle, intergranular fracture along grain boundaries. Conversely, the optimized post-treatment fracture surface displays an abundance of dimples and a few decohesive regions, indicating a shift from a brittle transgranular fracture mode to a mixed tough-brittle fracture mechanism.

3.2.2 Frictional wear

Figure 14 provides insights into the wear volume and friction coefficient of Y-modified ADC12 aluminum alloy before and after heat treatment. The data indicate that both the wear volume and friction coefficient experienced a post-treatment reduction, with the wear volume decreasing by 68.46 % and the friction coefficient by 4.80 %, compared to the pre-treatment values. This significant reduction demonstrates that the heat treatment notably enhances the wear resistance of the material. This improvement is likely due to the microstructural changes induced by the heat treatment, which typically include refinement and homogenization of phases within the alloy, contributing to its increased durability against wear and reduced friction in practical applications.

3.3 Results and discussion

During the solid solution treatment, the incipient Si dissolves extensively and spheroidizes. Although this

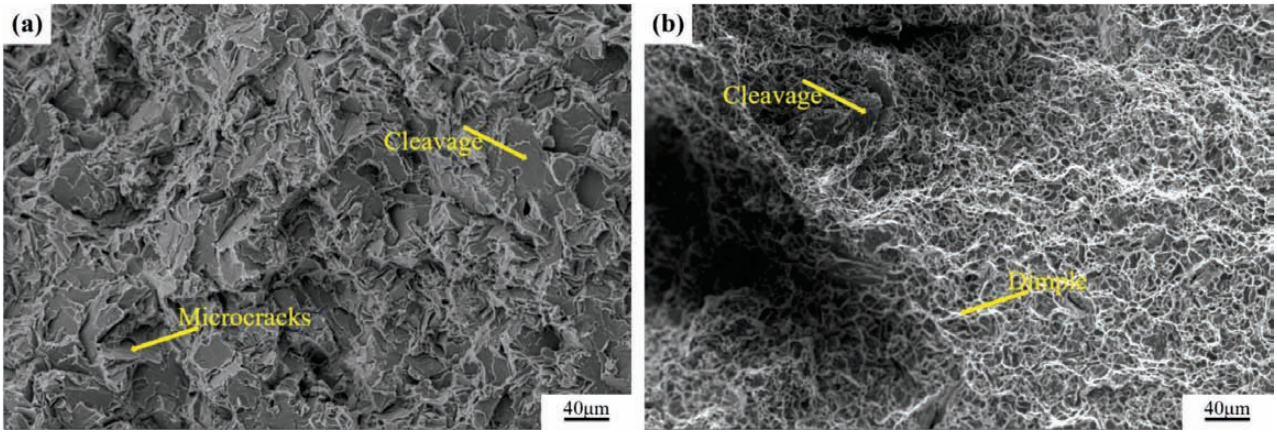

Figure 13: Fracture morphology of Y-modified ADC12 aluminum alloy before and after heat treatment: a) without heat treatment; b) validation experimental group

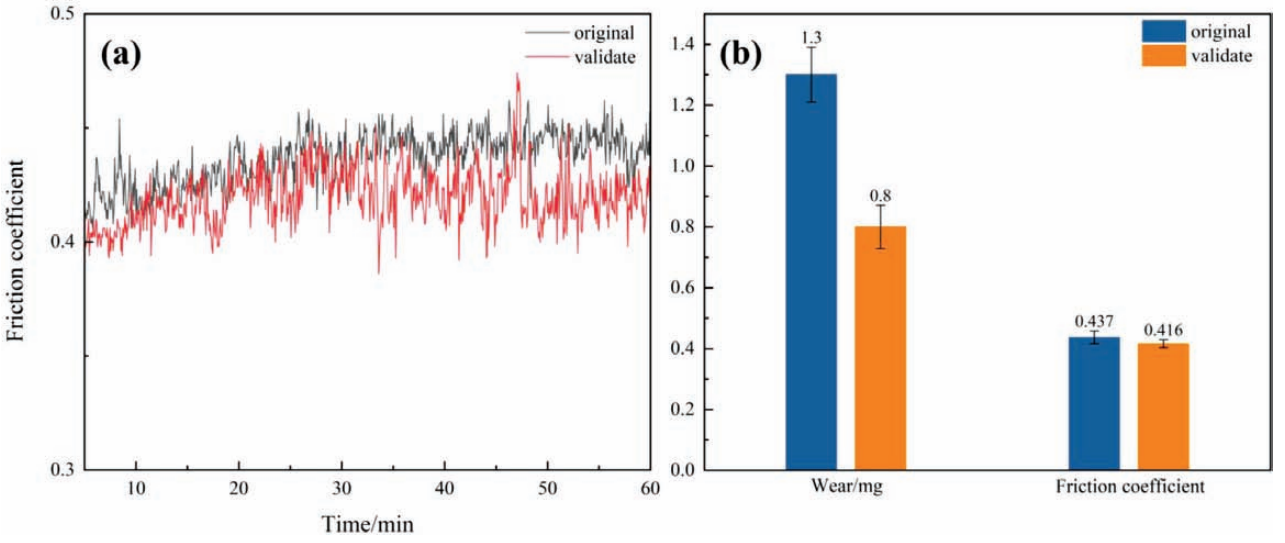

Figure 14: a) Friction curve of Y-modified ADC12 aluminum alloy before and after heat treatment; b) wear and friction coefficient of Y-modified ADC12 aluminum alloy before and after heat treatment

process is conducive to enhancing the alloy's strength, its impact is limited due to the minimal amount of incipient Si. Due to T6 heat treatment, the morphology of the eutectic Si phase undergoes significant transformations, including passivation, dissolution, spheroidization, and coarsening. These changes minimize the cutting effect of eutectic Si on the matrix, substantially improving the alloy's overall mechanical properties.[22,23] The eutectic Si, characterized by a higher content and denser distribution, markedly influences the alloy properties during the solid solution process. The coarse, flaky, and dendritic eutectic Si in the as-cast alloy, which cuts into the matrix, tends to generate stress concentrations at its sharp corners under load. However, the dissolution and spheroidization of eutectic Si during the solid solution process mitigate this cutting and reduce stress concentrations, thereby enhancing the alloy's strength. This morphological evolution of the Si phase improves the mechanical interaction between the hard particulate Si phase and the α-Al matrix.[24] Consequently, more complete and uniformly distributed eutectic Si spheroidization correlates with significant enhancements in mechanical properties. Solid solution treatment alters the eutectic Si phase, transforming elongated, fibrous structures into shorter rods or spheres. This optimization in morphology includes more rounded, smoother edges and contours, with a fine and homogeneous distribution of these particles along the grain boundaries. However, prolonged solid solution times can lead to coarsening of the eutectic Si phase.

The activation energy required for mutual diffusion between Si atoms and the α-A1matrix is considerably lower than that required along the Si interface[25,26] suggesting that mutual diffusion is the most probable mechanism for atomic migration in these materials. The relationship between the solid solution time and the size of Si atoms can be expressed with the following equation [27]:

$$dR/dT = -\Omega[D/R_0 + (D/\pi t)1/2]$$

Here, Ω is approximately the degree of supersaturation; D is the diffusion coefficient; R_0 is the initial size of Si atoms; and t is the time of solid solution treatment. Generally speaking, the die-cast ADC12 aluminum alloy initially exhibits a lamellar Si phase. Upon modification with rare earth element Y, the morphology of the Si phase transforms into fibrous or elongated structures. During heat treatment, the Si phase undergoes melting and spheroidization. Owing to the growth process occurring far from equilibrium, the alloy features intracrystalline twinning defects characterized by higher density and more branches, exhibiting a higher energy state. This condition facilitates the transformation of the Si phase into a crushable, fiber-like structure without melting, indicating a decrease in the initial size of Si atoms (R_0 value) and an increase in the dR/dT value, thereby reducing the solid solution treatment time. Given that the raw material for this experiment is ADC12 aluminum alloy, modified with rare earth Y via centrifugal casting, the original Si phase is already refined, necessitating a shorter solid solution treatment time compared to the parameters reported by C. Rungsinee et al.[13]

The objective of solid solution treatment is to enhance the plasticity and machinability of the alloy by dissolving unstable phases and dispersing them into the matrix. During this treatment, aluminum and copper atoms are rearranged to form Al2Cu, which dissolves into the aluminum matrix, impacting the mechanical properties. The solid solution treatment increases the rate and concentration of the Al_2Cu phase in the α-Al matrix, resulting in solid solution strengthening. However, it also eliminates segregation formed during non-equilibrium crystallization via diffusion. This homogenization improves the mechanical properties significantly.[28,29] The dissolution of Al_2Cu at grain boundaries in the as-cast

structure not only enhances interfacial strength but also allows for the precipitation of fine and dispersed Cu-containing particles during artificial aging, reinforcing the alloy matrix. The more complete the dissolution of Al_2Cu, the greater the strength of the alloy after heat treatment.

Following solid solution and artificial aging treatments, dispersed and small reinforcing phases precipitate within the alloy matrix, enhancing hardness and mechanical properties. During solid solution, both the Si and Al_2Cu phases dissolve to form a supersaturated solution, which decomposes during aging so that small, dispersed eutectic Si and Al-Cu intermediate phases precipitate, significantly strengthening the alloy's matrix. Compared to the Al_2Cu phase, the solid solubility of the Si phase is more restricted, likely due to the high silicon content in the alloy, which quickly reaches saturation at solid solution temperatures, slowing down the treatment process. The introduction of electromagnetic stirring[30] or a pre-deformation process[31] before heat treatment can reduce the Si phase size, elevate the solid solubility limit of the alloy, and further optimize mechanical properties.

4 CONCLUSIONS

(1) T6 heat treatment markedly enhances the microstructure and mechanical properties of Y-modified ADC12 recycled-aluminum alloy. Following the treatment, the dendritic α-Al phase nearly vanishes, transitioning into a more uniform distribution. Concurrently, the eutectic Si phase undergoes spheroidization, its size notably diminishes, and the α-Fe phase also decreases in size. With the optimal T6 heat treatment, significant reductions are observed: the area ratio of the eutectic Si phase decreases by 27.83 %, its average size by 57.89 %, and its average aspect ratio by 39.94 %. Additionally, the area ratio of the Al_2Cu phase drops by 97.26 %, underscoring the substantial impact of heat treatment on the solid solution of the eutectic Si and Al_2Cu phases. Furthermore, the average size of the α-Fe phase shrinks by 29 %, highlighting a remarkable refinement effect.

(2) The optimal T6 heat treatment parameters include a solid solution temperature of 520 °C for 7 h and artificial aging at 170 °C for 10 h. This treatment leads to significant improvements in the alloy's mechanical properties. The tensile strength increases from 186.39 MPa to 332.21 MPa, a 78.23 % rise; elongation increases from 7.5 % to 11.6 %, a 54.67 % increase; and the strength-to-plasticity ratio escalates from 1.398 GPa % to 3.851 GPa %, an increase of 175.46 %. Additionally, the coefficient of friction decreases by 4.80 %, and the wear is reduced by 68.46 %. The fracture mode transitions from brittle transgranular to mixed tough-brittle fracture, indicating a substantial improvement in the comprehensive mechanical properties of the alloy.

Acknowledgement

This work was financially supported by the Natural Science Foundation of Ningxia (2022AAC03256, 2024AAC03149), and Scientific research project of Ningxia Education Department (NYG2024075).

5 REFERENCES

[1] W. Jie-Fang, XIE Jing-Pei, L. Zhong-Xia, et al., Review on the Research and Application of Al-Si Piston Alloy at Home and Abroad, Foundry, 01 (**2005**), 24–27, doi:10.3321/j.issn:1001-4977.2005.01.006

[2] S. Farahany, A. Ourdjini, M. H. Idrsi, S. G. Shabestari, Evaluation of the effect of Bi, Sb, Sr and cooling condition on eutectic phases in an Al-Si-Cu alloy (ADC12) by in situ thermal analysis, Thermochimica Acta, 559 (**2013**), 59–68, doi:10.1016/j.tca.2013.02.024

[3] H. Xin, Y. Hong, Effect of trace La addition on the microstructure and mechanical property of as-cast ADC12 Al-alloy, Journal of Wuhan University of Technology (Materials Science Edition), 28 (**2013**) 01, 202–205, doi:CNKI:SUN:WLGY.0.2013-01-038

[4] K. A. Trowell, S. Goroshin, D. L. Frost, J. M. Bergthorson, Aluminum and its role as a recyclable, sustainable carrier of renewable energy, Applied Energy, 275 (**2020**), 115–112, doi:10.1016/j.apenergy.2020.115112

[5] D. Dudxinski, A. Devillez, A. Mouki, et al., A review of developmenls towards dry and high speed machining of Inconel 718 alloy, International Journal of Machine Tools & Manufacture, 44 (**2004**) 4, 439–456, doi:10.1016/S0890-6955(03)00159-7

[6] S. Aiping, Y. Yiming, Dual-carbon target brings new opportunities for recycled aluminum development, China Nonferrous Metals News, 2021-07-13(003)

[7] Q. Zhao, Z. Qian, X. Cui, et al., Optimizing microstructures of dilute Al-Fe-Si alloys designed with enhanced electrical conductivity and tensile strength, Journal of Alloys and Compounds, 650 (**2015**), 768–776, doi:10.1016/j.jallcom.2015.08.052

[8] S. Farahany, H. Ghandvar, On the effect of praseodymium on solidification characteristics, microstructure, and mechanical properties of commercial ADC12 alloy, Journal of Thermal Analysis and Calorimetry, 148 (**2023**) 12, 5247–5255, doi:10.1007/s10973-023-12073-9

[9] C. Puncreobutr, P. D. Lee, K. M. Kareh, et al., Influence of Fe-rich intermetallics on solidification defects in Al-Si-Cu alloys, Acta Materialia, 68 (**2014**), 42–51, doi:10.1016/j.actamat.2014.01.007

[10] C. Narducci, G. L. Brollo, R. H. M. de Siqueira, et al., Effect of Nb addition on the size and morphology of the β-Fe precipitates in recycled Al-Si alloys, Scientific Reports, 11 (**2021**) 1; 9613, doi:10.1016/j.jmatprotec.2015.03.011

[11] K. Abedi, M. Emamy, The effect of Fe, Mn and Sr on the microstructure and tensile properties of A356-10% SiC composite, Materials Science and Engineering: A, 527 (**2010**) 16–17, 3733–3740, doi:10.1016/j.msea.2010.03.063

[12] A. Jarco, J. Pezda, Effect of Heat Treatment Process and Optimization of its Parameters on Mechanical Properties and Microstructure of the AlSi11(Fe) Alloy, Materials (Basel), 14 (**2021**) 9, 2391, doi:10.3390/ma14092391

[13] C. Rungsinee, U. Ruethairat, W. Chanakarn, et al., The effects of heat treatment on microstructure and mechanical properties of rheocasting ADC12 aluminum alloy, Materials Today, 5 (**2018**) 3, 9476–9482, doi:10.1016/j.matpr.2017.10.127

[14] J. Xiong, H. Yan, S. Zhong, et al., Effects of Yb Addition on the Microstructure and Mechanical Properties of As-Cast ADC12 Alloy, Metals (Basel), 9 (**2019**) 1, 108, doi:10.3390/met9010108

[15] L. M. Wang, H. W. Wei, Z. J. Zhu, The effect of Y on the hot-tearing resistance of Al-5 wt.% Cu based alloy, Materials Design, 31 (**2010**), 2483–2487, doi:10.1016/j.matdes.2009.11.044

[16] H. Kailiang, C. Weiye, H. Hongming, et al., Effect of Casting Process on Microstructure and Mechanical Properties of ADC-12 Recycled Aluminum Alloy, Chinese Journal of Vacuum Science and Technology, 42 (**2022**) 6, 448–455, doi:10.13922/j.cnki.cjvst.202112016

[17] L. Ruijiang, Z. Yewang, W. Chongwei, et al., Study on the design and analysis methods of orthogonal experiment, Experimental Technology and Management, 27 (**2010**) 09, 52–55, doi:10.3969/j.issn.1002-4956.2010.09.016

[18] B. Jiabao, L. Zhibin, Y. Yongli, et al., Influence of T6 heat treatment on the microstructure and tribological properties of ADC12-GNPs composites, Diamond and Related Materials, 140, Part B (**2023**) 110497, doi:10.1016/j.diamond.2023.110497

[19] J. Liu, Q. Wu, H. Yan, et al., Effect of Trace Yttrium Addition and Heat Treatment on the Microstructure and Mechanical Properties of As-Cast ADC12 Aluminum Alloy, Applied Sciences, 9 (**2019**) 53, doi:10.3390/app9010053

[20] Z. Huang, H. Yan, Z. Wang, Microstructure and mechanical properties of strontium-modified ADC12 alloy processed by heat treatment, Journal of Central South University, 25 (**2018**), 1263–1273, doi:10.1007/s11771-018-3823-7

[21] B. Dang, Y. B. Li, F. Liu, Q. Zuo, M. C. Liu, Effect of T4 heat treatment on microstructure and hardness of A356 alloy refined by Ga-In-Sn mixed alloy, Materials Design, 57 (**2014**), 73–78, doi:10.1016/j.matdes.2013.12.022

[22] A. Forn, M. Baile, E. Martin, J. G. Sarriés, Heat Treatments Effect on A357 Components Produced by SSM, Solid State Phenomena, 116–117 (2**0**06), 181–184, doi:10.4028/www.scientific.net/SSP.116-117.181

[23] N. Growell, S. Shlvlcumar, Solution Heat Treatment Effects in Cast Al-Si-Cu Alloys, AFS Transactions, 103 (**1995**), 721–726, doi:10.1016/j.matdes.2009.10.035

[24] Y. Sun, J. Chen, G. X. Sun, Evolution of Si Phase in Al-Si Alloy and its Effect on Mechanical Properties, Nonferrous Alloys, 6 (**2001**), 1–4, doi:10.3321/j.issn:1001-2249.2001.06.001

[25] D. Bo, L. Cong-Cong, L. Feng, et al., Effect of as-solidified microstructure on subsequent solution-treatment process for A356 Al alloy, Trans. Nonferrous Met. Soc. China, 26 (**2016**), 634–642, doi:10.1016/S1003-6326(16)64152-3

[26] B. A. Howard, R. K. Gerald, Second phase dissolution, Metallurgical and Materials Transactions, 2 (**1971**) 2, 393–408, doi:10.1007/BF02663326

[27] L. Zhang, J. Gao, L. N. W. Darnoah, et al., Removal of Iron from Aluminum: A Review, Mineral Processing & Extractive Metallurgy Review, 33 (**2012**) 2, 99–157, doi:10.1080/08827508.2010.542211

[28] G. García-García, J. Espinoza-Cuadra, H. Mancha-Molinar, Copper content and cooling rate effects over second phase particles behavior in industrial aluminum-silicon alloy 319, Materials & Design, 28 (**2007**) 2, 428–433, doi:10.1016/j.matdes.2005.09.021

[29] Y. Yuying, Z. Sheng-Yi, C. Zhe, et al., Effect of Cr content and heat-treatment on the high temperature strength of eutectic Al-Si alloys, Journal of Alloys and Compounds, 647 (**2015**), 63–69, doi:10.1016/j.jallcom.2015.05.167

[30] L. Dehong, J. Yehua, G. Guisheng, Rongfeng Zhou, et al., Refinement of primary Si in hypereutectic Al-Si alloy by electromagnetic stirring, Journal of Materials Processing Technology, 189 (**2007**), 13–18, doi:10.1016/j.jmatprotec.2006.12.008

[31] J. He-miao, W. Xiao-yu, X. Xiang, et al., Effect of pre-deformation on microstructure and mechanical properties of 2024 aluminum alloy after thermomechanical treatment, Transactions of Materials and Heat Treatment, 44 (**2023**) 3, 68–76, doi:10.13289/j.issn.1009-6264.2022-0439